JOURNAL OF OCULAR PHARMACOLOGY AND THERAPEUTICS
Volume 37, Number 6, 2021

DOI: 10.1089/jop.2020.0140

Newly Identified Chemicals Preserve Mitochondrial Capacity and Decelerate Loss of Photoreceptor Cells in Murine Retinal Degeneration Models

Craig Beeson,[1] Yuri K. Peterson,[1] Nathan Perron,[2] Mausumi Bandyopadhyay,[2] Cecile Nasarre,[2] Gyda Beeson,[1] Richard F. Comer,[1] Christopher C. Lindsey,[1] Rick G. Schnellmann,[3,4] and Bärbel Rohrer[2,5]

Abstract

Purpose: Metabolic stress and associated mitochondrial dysfunction are implicated in retinal degeneration irrespective of the underlying cause. We identified seven unique chemicals from a Chembridge DiverSET screen and tested their protection against photoreceptor cell death in cell- and animal-based approaches.
Methods: Calcium overload (A23187) was triggered in 661W murine photoreceptor-derived cells, and changes in redox potential and real-time changes in cellular metabolism were assessed using the MTT and Seahorse Biosciences XF assay, respectively. Cheminformatics to compare structures, and biodistribution in the living pig eye aided in selection of the lead compound. *In-situ*, retinal organ cultures of rd1 mouse and S334ter-line-3 rat were tested, *in-vivo* the light-induced retinal degeneration in albino Balb/c mice was used, assessing photoreceptor cell numbers histologically.
Results: Of the seven chemicals, six were protective against A23187- and IBMX-induced loss of mitochondrial capacity, as measured by viability and respirometry in 661W cells. Cheminformatic analyses identified a unique pharmacophore with 6 physico-chemical features based on two compounds (CB11 and CB12). The protective efficacy of CB11 was further shown by reducing photoreceptor cell loss in retinal explants from two retinitis pigmentosa rodent models. Using eye drops, CB11 targeting to the pig retina was confirmed. The same eye drops decreased photoreceptor cell loss in light-stressed Balb/c mice.
Conclusions: New chemicals were identified that protect from mitochondrial damage and lead to improved mitochondrial function. Using *ex-vivo* and *in-vivo* models, CB11 decreased the loss of photoreceptor cells in murine models of retinal degeneration and may be effective as treatment for different retinal dystrophies.

Keywords: pharmacophore, ChemBridge library, calcium stress, retinitis pigmentosa, eye drops

Introduction

Retinitis Pigmentosa (RP) is an orphan disease that affects ~1 in 4,000 people worldwide, with mutations in over 50 genes involved in rod photoreceptor development, maintenance, and function.[1] Interestingly, irrespective of the underlying genetic mutation or the species studied, disruption in energy metabolism has been confirmed. For example, our group showed in 2 models of RP, the rd1 (phosphodiesterase 6 beta mutation[2]) and the rds mouse (peripherin mutation[3]), and the constant light damage model in Balb/c mice that metabolic genes, such as phosphofructokinase-1, the rate-limiting enzyme for glycolysis, is increased before the onset of degeneration and then drops as degeneration commences.[4] In addition, reduced retinal complex I activity (ie, oxidative phosphorylation) concomitant with oxidative stress was reported at stages before cell death in 4 mouse RP models, including the rd1 (retinal degeneration 1) and rds (retinal degeneration slow) mouse.[5]

Departments of [1]Drug Discovery and Biomedical Sciences and [2]Ophthalmology, Medical University of South Carolina, Charleston, South Carolina, USA.
[3]Department of Pharmacology and Toxicology, University of Arizona, Tucson, Arizona, USA.
[4]Research Service, Southern Arizona VA Healthcare System, Tucson, Arizona, USA.
[5]Research Service, Ralph H Johnson VA Medical Center, Charleston, South Carolina, USA.

Mitochondrial structure and function in ocular tissues appear to be altered in the aged eye,[6] in retinal dysfunction associated with Parkinson's disease,[7] in retinal diseases, including diabetic retinopathy and glaucoma,[8] and in age-related diseases such as age-related macular degeneration (AMD).[6,9–12] Thus, we hypothesized that early changes in energy metabolism underlie a number of photoreceptor dystrophies; and that agents, which ameliorate the dysregulation of energy metabolism, could be developed into therapeutic strategies for treatment of retinal degeneration.

In previous publications, we have shown that 661W cells (mouse retina-derived photoreceptor cells)[13] treated with the Ca^{2+}-ionophore A23187, nonhydrolyzable cGMP (8-Bromo-cGMP), or 3-isobutyl-1-methylxanthine (IBMX; phosphodiesterase inhibitor and adenosine receptor antagonist), mimic the pathological increase in Ca^{2+} influx seen in the rd1 mouse photoreceptors.[14] In the rd1 mouse, Ca^{2+} influx is due to the opening of cGMP-gated cation channels and is the best-characterized mouse model of RP.[2,15,16] Likewise, 661W cells challenged with hydroperoxides recapitulate many of the steps in cell death observed in the light-damaged albino mouse retina, a model for oxidative stress in RP and AMD.[17] Both the light damage and the rd1 mouse retina have been used to investigate neuroprotective therapies (see Wenzel et al.[18] for a comprehensive summary).

We have assessed the effects of excess calcium or oxidative stress on mitochondrial function indirectly in the intact mouse retina, and found that both rd1 retina and retina exposed to light damage exhibit high levels of stress and metabolic genes at the onset of damage and that metabolic genes dropped in parallel with the loss of cells.[4] Mitochondrial function has been assessed directly by measuring oxygen consumption levels, documenting a reduction in oxygen consumption in the wild-type retina in the presence of IBMX,[19] and in the rd1 retina when normalized to the mitochondrial content of the retina.[20]

The Seahorse Biosciences Instrument is a multiwell plate, high-resolution respirometric assay for measuring extracellular fluxes of metabolic acid extrusion (a measure of glycolysis) and oxygen consumption (a measure of oxidative phosphorylation).[21] A comparison was made among published data on metabolic alterations in RP models, which document a shift toward glycolysis before the onset of cell death,[4,22] and the Seahorse assays, where we showed a Warburg effect in metabolic responses to calcium or oxidant stress before succumbing to cell death in 661W cells.[23] For example, we showed that cell death at 24–48 h from a single high exposure to the Ca^{2+} ionophore A23184 or the oxidant tert-butyl hydroperoxide (tbuOOH) was correlated with the loss of mitochondrial capacity, estimated as the decrease in the maximal carbonyl cyanide-p-trifluoromethoxyphenylhydrazone (FCCP)-uncoupled rate, and was predictive of ensuing cell death.[23] Thus, we hypothesized that these early losses of mitochondrial integrity underlie retinal pathology and leads to loss of photoreceptor structure and function.

Our goal is to develop mitochondrial protective agents to mitigate RP, macular degeneration, and other retinal diseases. In unpublished experiments, we conducted a high-throughput screen using the thiazolium-formazan dye assay (MTT, primary endpoint assay) to measure protection against the A23187-induced calcium cytotoxicity and subsequent loss of metabolic capacity in the 661W cells. The ChemBridge DIVERset 50,000 chemical diversity small-molecule library was screened and resulted in the identification of 7 protective chemicals. In this study, our goal was to examine their efficacy and potency *in vitro*, identify a consensus pharmacophore, and to test the efficacy in *ex vivo* and *in vivo* models of RP.

Methods

Cells

Mouse retina-derived 661W photoreceptor cells were generously provided by Dr. Al-Ubaidi (University of Oklahoma)[13] and expanded in T75 flasks in Dulbecco's modified Eagle's medium (DMEM) +10% fetal bovine serum (FBS), plated in 100 mm tissue culture dishes and allowed to grow to 80%–90% confluence before harvesting for use in experiments.

Primary screen: calcium cytotoxicity

For the assay, 661W cells were seeded into each well of 96-well plates using DMEM supplemented with 5% FBS. Cells were grown to confluency for 48 h at which point the medium was replaced with DMEM +1% FBS. Seven compounds [CB1 (unique_ID 5122585), 2 (5404130), 3 (5404782), 6 (7606004), 10 (5677058), 11 (7630829), and 12 (7595333); ChemBridge, San Diego, CA] were added in concentrations of 0.1–10 μM, followed by the addition of the calcium ionophore A23187 [final concentration 1 μM and 3% dimethyl sulfoxide (DMSO)] 1 h later. After 24 h, cells were analyzed for redox capacity using the 3-(4,5-dimethylthiazol-2-yl)-2,5-diphenyltetrazolium bromide (MTT) assay. The MTT dye (1 mg/mL; Sigma-Aldrich) was added to each well and allowed to incubate overnight. The dark blue crystals formed were dissolved in 50 μL of 20% SDS (sodium dodecyl sulfate) in 0.01 M hydrochloric acid and the absorbance measured at 570 nm (background wavelength 650 nm) using Molecular Devices, SpectraMax 190 spectrophotometer (MDS Analytical Technologies, Toronto, ON, Canada). A23187 at 1 μM decreased the formazan dye signal ~50% at 24 h.[17,24] Results were analyzed as percent of vehicle absorbance.

Secondary screen: oxygen consumption rate

The oxygen consumption rate (OCR) measurements in 661W cells were performed using a Seahorse Bioscience XF96 instrument as previously reported.[23] O_2 leakage through the plastic sides and bottom of the plate was accounted for using the AKOS algorithm in the XF software package. Cells were plated on 96-well custom plates designed for use in the XF96 (typically 20,000 cells/well) and grown to ~90% confluency in DMEM +5% FBS (48 h). The medium was then replaced with DMEM +1% FBS for 24 h, along with any treatments. Before running the experiment, the growth medium was removed and the cells were washed with phosphate-buffered saline (PBS) containing Ca^{2+}/Mg^{2+} (pH 7.4), which was then aspirated and replaced with 700 μL of bicarbonate-free DMEM buffer. The buffer contained $CaCl_2$ (1.8 mM), $MgCl_2$ (0.6 mM), KH_2PO_4 (0.5 mM), KCl (6.3 mM), Na_2HPO_4 (0.5 mM), NaCl (135 mM), glucose (5.6 mM), 1 mM glutamine, minimum essential medium (MEM) amino acids solution, MEM

nonessential amino acids, MEM vitamin solution, penicillin/streptomycin, 1% bovine serum albumin (factor V fatty-acid-free), 1% FBS, and insulin (100 nM). OCR measurements were obtained every 5 min, collecting 3 measurements per well at baseline and 3 measurements upon injection of the protonophore FCCP (1 μM), which collapses the proton gradient across the inner mitochondrial membrane and increases maximal electron transport chain oxygen consumption. The data were normalized to the number of cells on the plate as identified by DAPI and imaged using the INcell 1000 cellular imaging system (GE Healthcare).

Tertiary screen: organ cultures

Rd1 mice were generously provided by Deborah Farber (UCLA, Los Angeles, CA)[25] and the S334ter-line-3 rat was obtained from Mathew LaVail (UCSF, San Francisco, CA).[26] The mice were housed in the Medical University of South Carolina (MUSC) Animal Care Facility under a 12-h light/12-h dark cycle, with access to food and water *ad libitum*. All experiments were performed in accordance with the ARVO Statement for the Use of Animals in Ophthalmic and Vision Research and were approved by the MUSC Animal Care and Use Committee. All chemicals used for organ cultures were tissue culture grade and were purchased from Invitrogen (Carlsbad, CA). Retina-RPE (retinal pigment epithelium) cultures were grown using the interface technique according to published protocols[27–29] with modifications.[30] All preparations were performed under a laminar flow hood. Pups were deeply anesthetized by hypothermia and decapitated. Heads were rinsed in 70% ethanol and eyes collected and placed in ice-cold Hanks balanced salt solution plus glucose (6.5 g/L). To collect the retina with RPE attached, eyes were incubated in 1 mL of media containing cysteine (0.035 mg) and papain (20 U) at 37°C for 15 min. Enzymatic activity was stopped by adding media plus 10% fetal calf serum. The anterior chamber was removed, followed by the lens and vitreous. Using a pair of #5 forceps, the retina with the RPE attached was then carefully dissected free from the choroid and sclera. Relaxing cuts were made into the retina-RPE sandwich to flatten the tissues. The tissues were then transferred to the upper compartment of a Costar Transwell chamber using a drop of Neurobasal medium (Invitrogen), RPE layer face down. A drop of fluid was used to flatten out the tissue, by gently spreading the drop of liquid with the fused end of a glass Pasteur pipette. Neurobasal media supplemented with 1% N1, and 2% B-27 supplements were placed in the lower compartment. The cultures were kept in an incubator (5% CO_2, balanced air, 100% humidity, at 37°C). The medium was changed every 2 days. No antimicrobials or antibiotics were included. After completion of the experiment, retina cultures were fixed in 4% paraformaldehyde (PFA). Tissues were cryoprotected in 30% sucrose, frozen in TissueTek O.C.T. (Fisher Scientific, Waltham, MA), cut into 14 μm cryostat sections, and stained with Toluidine Blue. Rows of photoreceptors were counted in 4 regions of the retina, and an average was obtained across the retina.[31]

Molecular modeling

Compounds were first clustered using Atom Pair descriptors and Tanimoto coefficient averaged link hierarchical clustering using ChemMine and visualized using Dendrocope.[32] CB11 and CB12 were then analyzed to create a pharmacophore model using Molecular Operating Environment (MOE) by Chemical Computing Group, Inc. (MOE, 2019.01; Chemical Computing Group ULC, Montreal, QC, Canada). Automated 2D and 3D alignment was performed but did not yield quality models. Knowledge-guided modeling building was performed where molecules were manually aligned in 2D then flexibly refined in 3D to maximize overlap of similar physicochemical features. Features were then defined as having 100% consensus between molecules using the pharmacophore elucidation function in MOE.

In vivo *testing*

Retinal degeneration in RP caused by genetic defects involves oxidative and calcium stress, leading to rod cell death by apoptosis. Retinal damage due to constant light exposure also triggers rod photoreceptor degeneration due to apoptosis, making it a popular model for pathway analysis and drug discovery.[18] Light exposure experiments were performed on 3-month-old Balb/c mice. Light exposure consisted of constant fluorescent illumination of ~150–175 ft-c for 10 days as described previously,[31] ensuring that all cages were equidistant to the light source. Light was provided by two 30-W fluorescent bulbs (T30T12-CW-RS; General Electric, Piscataway, NJ) suspended ~40 cm above the cages, and light intensity was measured using a light meter (Extech Instruments, Waltham, MA). This amount of light reduces the number of rods by 50% within 10 days in albino mice. After completion of the experiment, eyes were fixed in 4% PFA and processed for histology and cell counts as above for retinal organ cultures.

Retinal bioavailability

MUSC made available a swine used for training purposes while under anesthesia[33] for tissue procurement. CB11-containing eye drops (1 mM final concentration) were generated in 0.9% NaCl, solubilizing CB11 in 100% ethanol and added to a 1.4% final concentration of ethanol with 0.5% Brij-78 [polyoxyethylene(20) stearyl ether] as a surfactant; 0.9% NaCl with 1.4% final concentration of ethanol and 0.5% Brij-78 served as the vehicle control. Eye drops were given bilaterally every 30 min for ~2 h ($n=4$) before euthanasia by the veterinary staff, comparing CB11 versus vehicle control. After euthanasia, eyes were enucleated, washed carefully in PBS to remove any remaining eye drops, wrapped in tin foil and snap-frozen in liquid nitrogen.[34] While still frozen, and on a bed of dry ice, the anterior chamber was removed and the lens was carefully lifted out of the eye cup. The intact frozen vitreous body was subsequently removed, leaving the empty eye cup from which retina was peeled off. Retinas were lyophilized for 48 h, taken up in 2 mL of PBS (pH 7.4) by vortexing and spiked with celecoxib (10 μL of 52.4 μM), as an internal standard to determine extraction efficiency, and extracted with 6 mL of dichloromethane/ethyl acetate (1:1). The sample was centrifuged (15 min at 5,500 rpm at 10°C), the organic layer separated and lyophilized, and re-extracted using the same procedure. The residual was lyophilized and brought up in 500 μL 80:20 acetonitrile:water, filtered through a 45 μm filter, and analyzed using an Agilent

1100-Agilent 6250 quadrapole MS, using a Kinetex column (Phenomenex, 50 × 2.1 mm, 100 Å, C18), injecting 5 μL sample in 15 min of 5–100% acetonitrile (MeCN). API ionization and single ion mode (SIM) detection optimized to CB11 (*m/z* 325), CB11 + H_2O (*m/z* 307), and celecoxib (*m/z* 381) was used. The estimated sensitivity was 0.05 ng/μL.[34] The amount of CB11 in the retina was calculated from the SIM-measured total ion count area determined from linear regression of the calibration curve, and adjusted for retina volume. Volume was based on area of retina (1.094 cm^2) and its average thickness (250 μm) (webvision.med.utah.edu).

Statistics

For data consisting of multiple groups, 1-way ANOVA followed by Fisher's *post hoc* test ($P < 0.05$) was used, and *post hoc* tests were run only if F achieved $P < 0.05$; single comparisons were analyzed by *t*-test analysis ($P < 0.05$), using Prism (GraphPad, San Diego CA) and StatView (SAS Institute, Cary NC) software.

Results

Chemical entities

We previously identified 7 active chemical entities from the ChemBridge DIVERset 50,000 chemical diversity small-molecule library that provided protection against calcium-mediated cell toxicity in 2 cell lines from 2 different species (mouse and rat), both of neuroectoderm lineage (photoreceptor and glia) (Fig. 1A). The cladogram of the hits is based on average distances as measured through Tanimoto coefficients between 0.4 and 0.6 (Fig. 1B) and visual inspection (Fig. 1A).[35] In general, the compounds are not related to each other chemically. CB1 and CB2 cluster due to both having a 1,1 dimethyl, whereas CB6 and CB11 cluster due to having a 4-carbon alkane. None of the compounds was obvious redox agents, metal ion chelators, or in the Pan-Assay INterference CompoundS (PAINS) category, although CB1 contains a strong electrophilic nitrile group.

Preservation of metabolic capacity in response to calcium stress (MTT assay)

To mimic elevated calcium in RP,[15] 611W cells were treated with A23187 at a concentration selected to result in a 50% decrease in metabolic reduction of thiazolium salts (MTT activity of 0.5; Fig. 2). While these assays are commonly used to measure cell viability, they actually assay oxidoreductase activities that use NAD(P)H as a reductant.[36] In this study, we refer to the readouts of these assays as a measure of ''metabolic capacity.'' Cells were pretreated with the CB chemicals for 1 h followed by addition of A23187 (1 μM). After 24 h, thiazolium dye was added and the conversion to formazan dye measured. The concentration responses for the compounds were scaled between MTT activity of 0.5 (A23187+DMSO vehicle) and 1 (DMSO vehicle alone). Six compounds (CB1, 2, 6, 10, 11, 12) protected against the loss of metabolic capacity in a concentration-dependent manner with ~80 efficacy. CB3 did not exhibit any protection.

Preservation of metabolic capacity in response to calcium stress (Seahorse assay)

The Seahorse XF96 respirometry assay has been used previously by us and others to analyze bioenergetic metabolism.[23] In previous experiments, we have utilized IBMX to induce calcium-mediated cell injury in 661W photoreceptors.[24] Two measurements were obtained, basal respiration and maximal respiratory capacity. The level of basal respiration was measured after equilibrating the cells in the XF DMEM media; mitochondrial maximal capacity was determined after exposing the cells to a protonophore FCCP, thereby uncoupling ATP production and leading to maximal oxygen consumption. Exposure of cells to IBMX for 24 h reduced FCCP uncoupled respiration by ~50%[23] (Fig. 3). Pretreatment of the 661W cells for 1 h with CB1, 2, 3, 6, 10, 11, and 12 (1 μM) before IBMX exposure for 24 h improved the uncoupled OCR rates for all compounds, except CB3. Overall, the active compounds were equally efficacious and improved respiration.

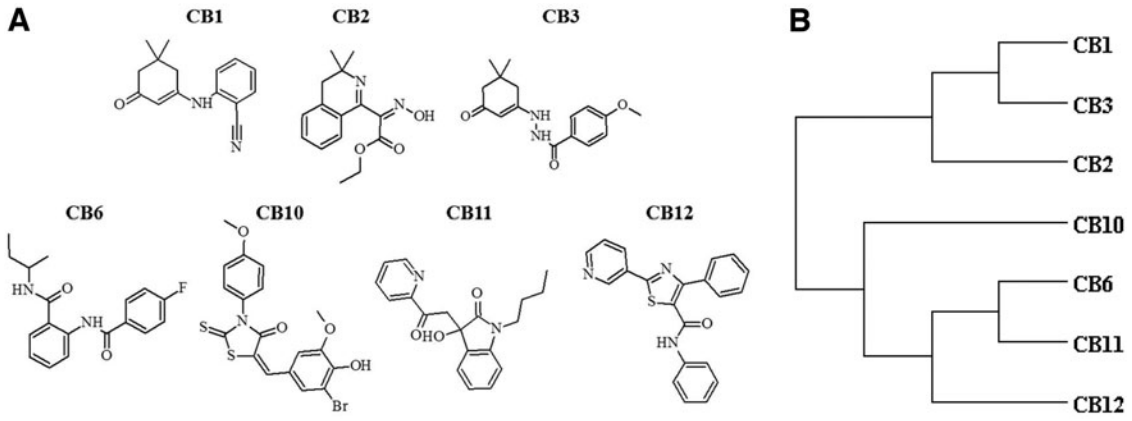

FIG. 1. Structure and similarities between initial hit compounds. Initial hits from the screen for protection of metabolic capacity from calcium-induced stress exhibit high structural diversity. Shown in **(A)** are the chemical graphs of the 7 initial active hits. Shown in **(B)** is a cladogram of the 7 initial hits based on average similarity distances as measured through atom-pair Tanimoto coefficients.

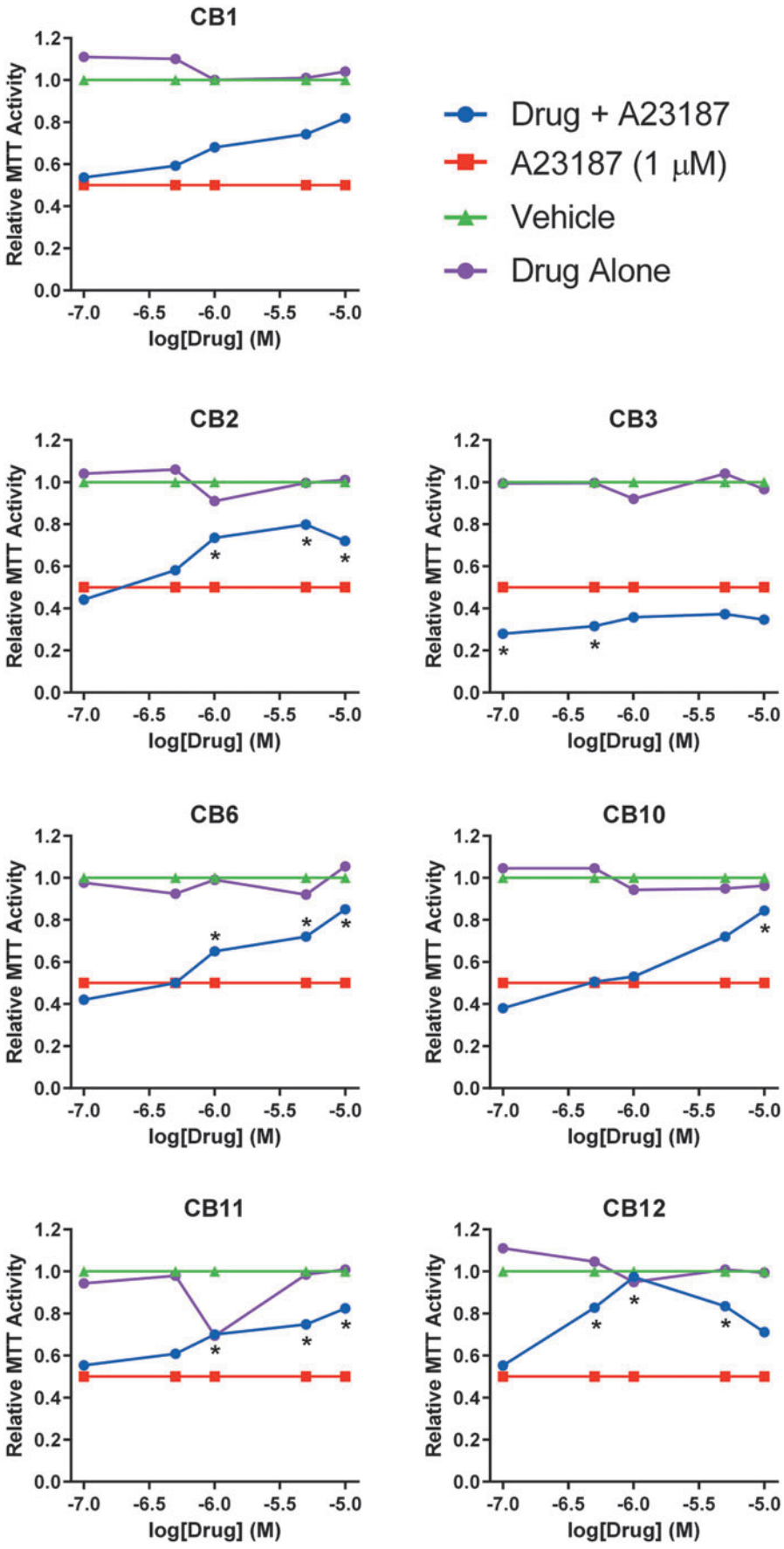

FIG. 2. Protection against calcium cytotoxicity. 661W cells seeded in 96-well plates were treated with calcium ionophore A23187 (final concentration 1 μM and 3% DMSO) to produce 50% cell death after 24 h (*red* traces). Seven compounds (CB1, 2, 3, 6, 10, 11, 12; ChemBridge, San Diego, CA) were added in concentrations of 0.1–10 μM (*blue* traces) and tested for efficacy using the MTT assay. Vehicle alone (*green* traces) or compounds alone (*purple* traces) had no effect on cell survival. Data represent mean per group and statistical significance (A23187 vs. drug+A23187, $*P < 0.05$) is indicated. DMSO, dimethyl sulfoxide; MTT, 3-(4,5-dimethylthiazol-2-yl)-2,5-diphenyltetrazolium bromide.

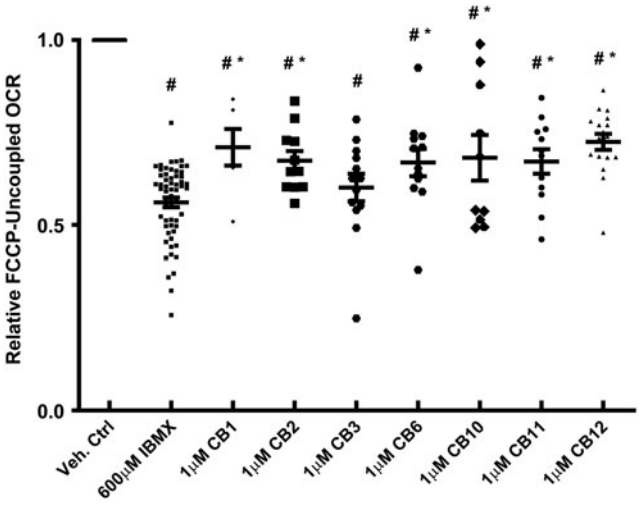

FIG. 3. 661W mitochondrial respiration is preserved by protective agents. The OCR and ECAR of 661W cells were measured with an XF96 Seahorse Biosciences instrument. The media is DMEM with 5.5 mM glucose; and the rates have been normalized to milligram of protein. After measuring several basal rates, the cells were treated with FCCP (1 μM) to determine maximal respiratory capacity. Shown are the average rates ± SEM and individual data points. Vehicle control rates were set to 100%, IBMX as a stressor reduced the relative FCCP uncoupled OCR by ~50%. All compounds significantly increased maximal respiratory capacity. Statistical significance (IBMX vs. drug, $^{\#}P < 0.05$ and control vs. drug, $^{*}P < 0.05$) is indicated. DMEM, Dulbecco's modified Eagle's medium; ECAR, extracellular acidification rates; FCCP, carbonyl cyanide-p-trifluoromethoxyphenylhydrazone; IBMX, 3-isobutyl-1-methylxanthine; OCR, O_2 consumption rates; SEM, standard error of the mean.

Identification of a pharmacophore

The 6 active compounds are structurally distinct members with a chemical similarity <40% (Fig. 1B). The lack of similarity in chemical space compelled us to use pharmacophore modeling to extract similar molecular features among the compounds, as we assumed there was a similar target. While automated pairwise alignment of pharmacophore features failed to find more than 3 consensus features; manual alignment of chemical pairs using pharmacophore elucidation features as a guide[37,38] was successful for CB11 and CB12 (Fig. 4). Compounds were aligned manually first in 2 and then minimized in 3 dimensions based on the presence of consensus chemical features within both of the compounds to maximize overlap of similar physicochemical features, and minimizing collective volume.

The CB11/CB12 pharmacophore modeled all of the possible bonding features within the 2 compounds. Seven total features with tight volumes were identified, with the maximum distance between features being 9.7 Å. The 7 physicochemical features are represented by 2 proton acceptors, 2 aromatics, 1 hydrophobic, 1 mixed proton donor/hydrophobic, and a feature that could include either a hydrophobic/acceptor feature that represents the pyridine and was the largest diameter feature to include the nitrogen (Fig. 4). The pharmacophore only matches with CB11 and CB12 when all 7 features are required.

We then took a closer look at the physiochemical properties of CB11 and CB12. Both CB11 and CB12 do not violate Lipinksi Ghose, Veber, Egan, or Muegge drug likeness rules. CB11 has a better topological polar surface area (TPSA), smaller mass, is more soluble, and in particular has a higher degree of saturation and therefore is more permeant to the blood/brain barrier than CB12. Lipophilicity or octanol/water partition coefficient (cLogP) and aqueous solubility (cLogS) are considered, as they affect absorption and distribution characteristics. A drug targeting the central nervous system (CNS) ideally has a logP value around 2[39] and logS value greater than −4 and CNS-multiparameter optimization (MPO) >4. Based on the more ideal estimated parameters for CB11 (cLogP: 2.30; cLogS: −3.73, TPSA: 70.5 Å^2 CNS-MPO: 5.70, MW: 324.4) versus CB12 (cLogP: 4.06; cLogS: −5.84 TPSA: 83.1 Å^2 CNS-MPO: 3.99, MW: 357.4), we chose to test CB11 in animal models.

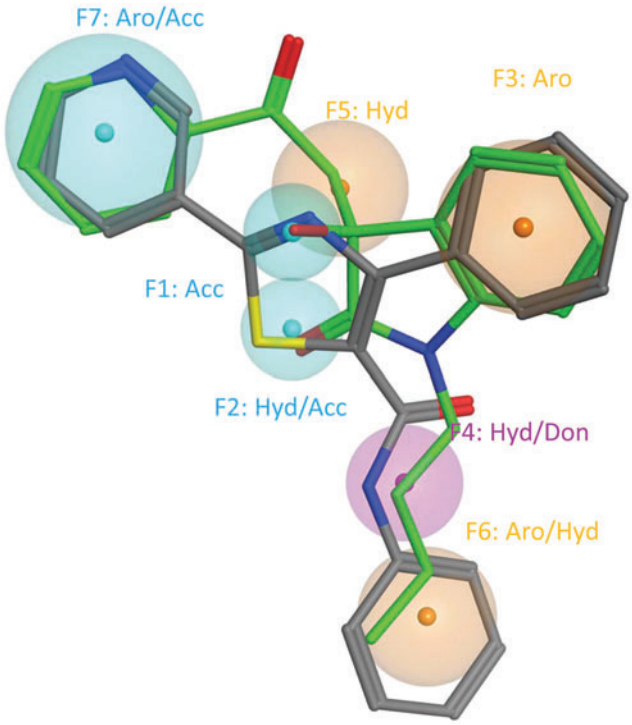

FIG. 4. The best leads define a single pharmacophore. Shown is a 7-feature pharmacophore model overlaid on the structural alignment of CB11 and CB12. Consensus physicochemical features are represented as spheroids where the smaller diameter indicates more concise overlap. CB11 is shown in *green* and CB12 in *gray*. Features with proton donor properties are colored *blue*, donor in *purple*, and hydrophobic in brown. Seven total features with tight volumes were identified, with the maximum distance between features being 9.7 Å. The physicochemical features are represented by 2 proton acceptors, 2 aromatics (Aro), 1 hydrophobic (Hyd), 1 mixed proton donor (Don)/hydrophobic, and a mixed hydrophobic/proton acceptor (Acc) feature.

Protection in mouse and rat organ cultures

Retinal explants are a powerful *ex vivo* screening tool[40] that allows the testing of photoreceptor cell survival within an *in vitro* retinal system that closely mimics the *in vivo* environment. We utilized 2 species that include 2 different genetic mutations known to be involved in RP. The genotype of the rd1 mouse[2] is a mutation in the β-subunit of the phosphodiesterase gene. This mutation results in high levels

of cGMP[15] and increased cGMP-gated channels in the open state enabling intracellular calcium to rise to toxic levels and cause rapid rod degeneration.[16] The genetic deficit and the retinal pathology is very similar to that observed in patients with βPDE-dependent RP. In these mice, rod photoreceptor degeneration starts after postnatal day 10 (P10), progressing rapidly, such that at P21 only 1–2 rows of the 7 initial rows of photoreceptors remain, mainly representing cones. Finally, the rd1 mouse retina cultures replicate both retinal development and degeneration, following the same time course as *in vivo*.[28]

The second model is the S334ter rhodopsin transgenic rat (line 3) that degenerates very rapidly.[26] Similar to the rd1 mouse, rod photoreceptor degeneration in the S334ter rats starts after P11, progressing rapidly with a minimal number of rows remaining by P21.[41] These rats overexpress a mouse opsin transgene with a termination codon at residue S334 (S334ter). Importantly, this C-terminal truncation leads to the elimination of all the phosphorylation sites[42] as well as the rhodopsin trafficking domain.[43]

The rd1 retinal explants were cultured for 11 days *ex vivo* (harvested on day P10) and the S334ter rhodopsin transgenic rat retinal explants were cultured for 6 days (harvested on day P12). Explants were treated with CB11 (1 μM) added to fresh medium every alternate day and the rows of photoreceptors remaining in the outer nuclear layer (ONL) counted (Fig. 5B).

Rd1 explants grown in culture for 12 days and treated with vehicle only contained 1.2 ± 0.2 cells in the ONL; cultures treated with CB11 contained 3.2 ± 0.2 cells in the ONL. Experiments were repeated in S334ter explants using CB11 (1 μM). S334ter explants grown in culture for 6 days and treated with vehicle were found to contain 2.0 ± 0.2 cells in the ONL (Fig. 5C), whereas treatment with CB11 increased that number to 3.9 ± 0.4.

Ocular bioavailability of CB11 and in vivo *protection in mouse model of light damage*

The cLogP and LogSW of CB11 suggested that it may be bioavailable in the retina after topical administration. To generate preliminary bioavailability data, a swine, while under anesthesia,[33] was given bilateral eye drops (vehicle vs. CB11) 2 h before euthanasia. Eyes were enucleated, snap frozen in liquid nitrogen and dissected.[34] Retina samples were solubilized, the CB11 sample was spiked with celecoxib, and both CB11 and PBS samples were extracted with ethyl acetate and levels of CB11 determined by SIM

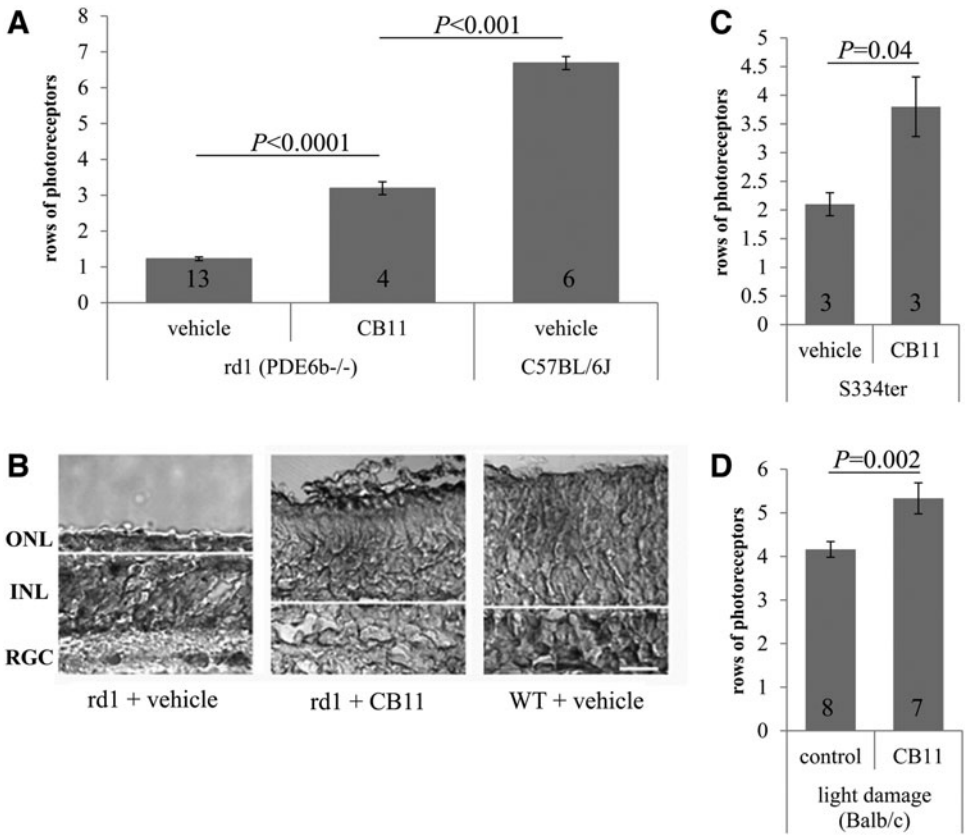

FIG. 5. CB11 is protective in mouse models of retinal degeneration. Neuroprotection against retinal degeneration was tested *ex vivo* on organ cultures **(A–C)** and *in vivo* **(B)**. **(A)** Rod photoreceptor cell survival was improved ~3-fold in rd1 organ cultures treated with CB11 when compared with controls. Vehicle-treated C57BL/6J WT mice were used as controls. **(B)** Examples of organ cultures are shown. ONL (photoreceptors), INL, RGC, and the border between photoreceptors and INL (*white* line) are identified for orientation. **(C)** Rod photoreceptor cell survival was improved ~2-fold in S344ter rhodopsin transgenic rat organ cultures treated with CB11 when compared with controls. **(D)** The number of rows of photoreceptor was improved by CB11 *in vivo* in mice exposed to white light to induce photoreceptor degeneration. Data represent mean ± SEM and number of animals, as well as statistical significance are indicated. INL, inner nuclear layer; ONL, outer nuclear layer; rd1, retinal degeneration 1; RGC, retinal ganglion cells; WT, wild type.

detection through liquid chromatography–mass spectrometry (LC-MS) (Fig. 6). Celecoxib (Fig. 6C) was used to confirm >95% extraction efficiency of compounds from the retina (Fig. 6B). CB11-specific peaks were absent in samples from eyes treated with PBS (Fig. 6D), confirming lack of transfer of drug to the contralateral eye over the 2-h treatment period. The concentration determined for CB11 delivered by 4 eye drops was $\sim$4.6 μM in the porcine retina.

Rod photoreceptors in Balb/c mice are susceptible to light-induced cell death,[31,44] leading to cell death due to apoptosis, the common pathway seen in RP. This commonality makes it a popular model to screen for neuroprotective

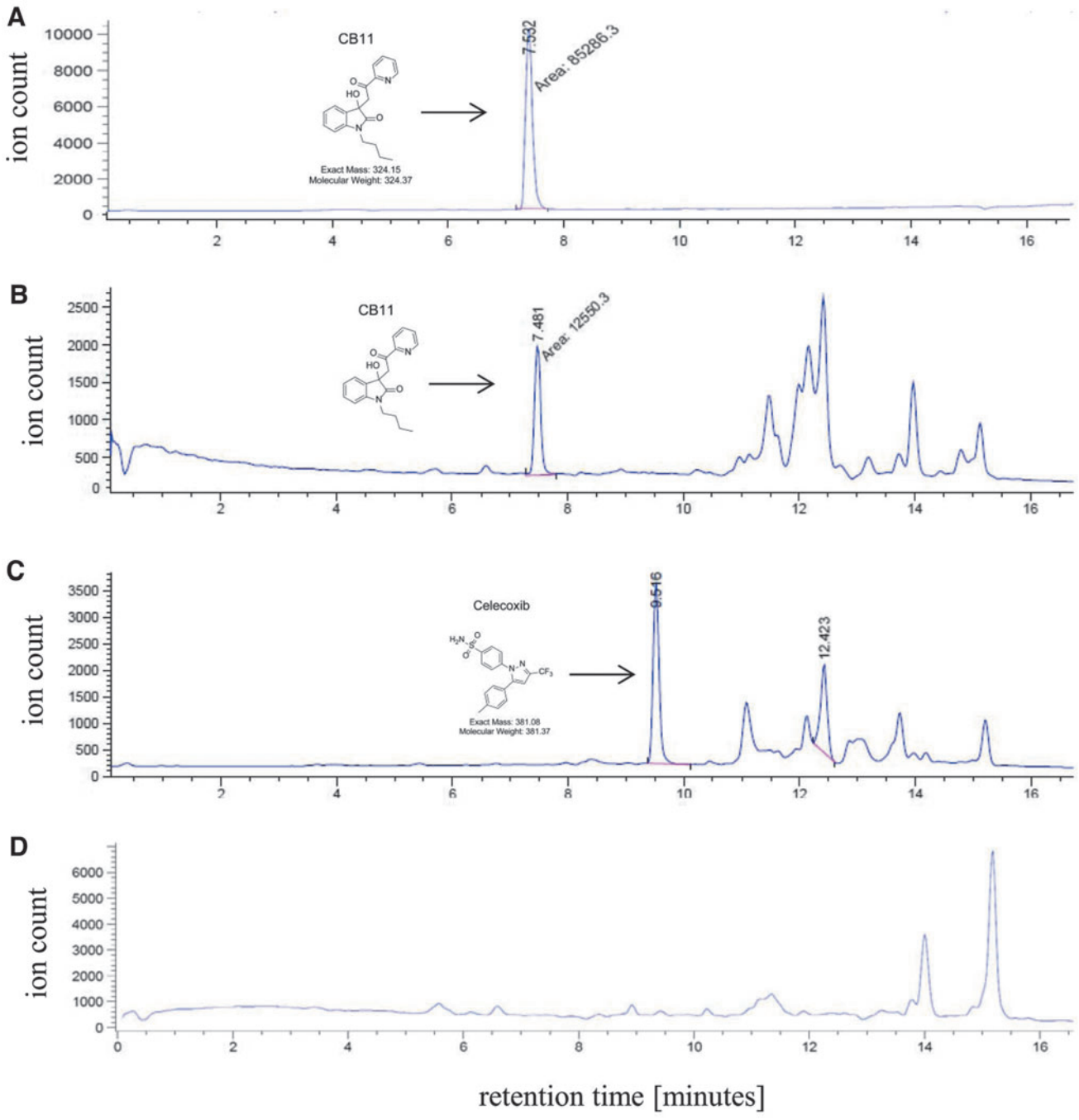

FIG. 6. Bioavailability of CB11 in porcine retina. CB11 was administered through eye drops to an anesthetized animal 2 h before euthanasia/enucleation, followed by tissue collection, and bioanalytical extraction. Retina sample from the CB11-treated eye was spiked with celecoxib to determine extraction efficiency, and concentrations of CB11 and celecoxib were determined when compared with CB11 standard. LC-MS SIM chromatograms are shown for all traces. LC-MS traces are shown for pure CB11 standard **(A)**, the retina sample from the eye treated with CB11 **(B)**, and its corresponding celecoxib signature **(C)**, and a retina sample from the eye treated with PBS only and imaged in SIM for CB11 **(D)**. Please note that the additional peaks at 11 min and beyond are complex biochemical fragments of unknown origin. LC-MS, liquid chromatography–mass spectrometry; PBS, phosphate-buffered saline; SIM, single ion mode.

strategies.[18,45] The number of rows of photoreceptor nuclei were counted in 10 equidistant locations across the entire retina, which were averaged to provide a single value for the entire retina.[31] After 10 days of light exposure, the number of rows of photoreceptors per total retina in vehicle-treated mice was 4.2 ± 0.2 (Fig. 5D), whereas animals treated with daily CB11 had 5.3 ± 0.4 rows remaining.

Discussion

The genesis of our program to identify metabolic neuroprotectants was based on our previously published observation that calcium or oxidative stress causes a rapid loss in maximal mitochondrial capacity in 661W cells as measured by respirometry, and that the degree of loss in maximal capacity was predictive of subsequent cell death measured.[23] Our rationale was that a primary screen focused on metabolic capacity (MTT assay) would rapidly identify potential cytoprotective agents that we could follow up with secondary and tertiary screens focused to specifically target the metabolic phenotype related to photoreceptor cell degeneration. A preliminary excerpt was published previously as part of a conference proceeding.[46]

Following this strategy, the main results of the current study are: (1) utilizing the 661W cone photoreceptor-derived cells and MTT and maximal oxygen consumption assays, 6 compounds from the 50,000 compound ChemBridge library protected against dysregulated energy metabolism triggered by calcium stress; (2) a pharmacophore, uniquely describing common features of CB11 and CB12 was identified; (3) CB11 was found to slow the progression of photoreceptor cell loss in the rd1 mouse organ culture; (4) CB11 was also tested in the S334ter rhodopsin rat retina organ culture, confirming efficacy across species and genetic phenotypes underlying degeneration; (5) Preliminary bioavailability of CB11 in the pig retina suggests that pharmacological concentrations can be achieved upon eye drop application; and (6) CB11 efficacy was confirmed in the light-induced retinal degeneration model in the Balb/c mouse.

Mitochondrial dysfunction is a common feature in most neurodegenerative diseases. While the mitochondria are typically known to produce ATP, other mitochondrial functions include the protection from reactive oxygen species (ROS) and calcium buffering. Six out of the 7 compounds from the ChemBridge library protected against dysregulation of energy metabolism triggered by calcium and oxidant stress, as measured using the MTT and maximal oxygen consumption assays. While the structural disparities are facilitated by the cladogram (Fig. 1B), 2 compounds, CB1 and CB3, merit some discussion. It was originally postulated that the structural commonalities of these compounds, the geminal dimethyl cyclohexenone core, should afford a conserved protective effect for both CB1 and CB3; yet, CB1 was effective while CB3 was not. However, it would be difficult to appreciate the precise reason for this outcome without the aid of an X-ray crystal structure of CB1 or CB3 bound to its target.

Pharmacophore modeling to identify similar molecular features among the compounds was pursued, assuming that they were recognizing a similar target. Manual alignment of chemical pairs using pharmacophore elucidation features as a guide[37,38] was successful for CB11 and CB12. The CB11/CB12 pharmacophore modeled all of the possible bonding features within the 2 compounds, identifying 7 total features with tight volumes and maximum distance between features of 9.7 Å. The 7 physicochemical features of the pharmacophore suggest a specific biochemical interaction with its targets, and fit within all common drug likeness rules. CB11 is expected to be more permeant to the blood/retina barrier, based on TPSA, smaller mass, greater solubility, and higher degree of saturation. Based on these analyses, CB11 was selected as the lead candidate for further *ex vivo* and *in vivo* analyses.

We and others have shown that the rodent retina recapitulates development and degeneration *in vitro*, and can hence be used as an *ex vivo* screening tool for neuroprotective agents.[40] Our data showed that CB11 was found to be protective in 2 species (mouse and rat) and 2 different genetic mutations (*βPDE6*,[2] and S334ter rhodopsin[26]), confirming efficacy across species and genetic phenotypes underlying degeneration. Specifically, these 2 models were chosen since they geno- and phenocopy the human RP, and degeneration occurs over the time course amenable to growth in organ cultures. CB11 in the S334ter rhodopsin rat improved survival by 2-fold, from $\sim$2 to $\sim$4 rows, in rd1 mouse by $\sim$3-fold from 1 to 3 rows of cells. The rd1 mouse has previously been used in organ cultures, with dopamine receptor inhibition improving cell survival by $\sim$3-fold.[40]

Bioavailability of CB11 in the retina was confirmed in the pig eye using eye drop application. Extraction efficiency of compound from porcine eye samples was aided by adding a known quantity of celecoxib. This reagent was chosen due to its physical characteristics (including strong ultraviolet activity), difference in retention time on LC-MS used for the experiment, and established stability under the developed extraction method (unpublished data). The pig was chosen for its larger eye size that affords greater ease to isolate the different layers without crosscontamination, as well as for its greater relevancy to the human condition for future studies.[47] Having confirmed that CB11 was observed in the retina after topical delivery, CB11 efficacy was tested in the Balb/c light damage model. This model was chosen since it has been used by many researchers in the context of neuroprotection and is a model of retinal degeneration due to apoptosis, including RP and AMD.[18] Approximately, 1.5 rows of photoreceptors across the dorsal and ventral retina were retained with CB11 treatment. We argue that protection of 1.5 rows of photoreceptors is meaningful. First, since we have not optimized the dose, dosing protocol, and dosing length, the protection of photoreceptors could be greater. Second, CB11 should be tested in other models of retinal degeneration. Third, Paquet-Durand and colleagues reported a maximal photoreceptor cell rescue of $\sim$40% in the rd1 mouse even when all calcium influx through the calcium channel of the photoreceptor outer segment membrane, which is thought to be the main driver of degeneration, which was genetically eliminated (rd1 $\times$ *Cngb1*$^{-/-}$).[48] Likewise, protection in the light damage model by growth factors seems to be limited to a few rows.[49]

The idea of targeting mitochondria for therapy to prevent retinal degeneration has been examined. The typical approach is to utilize molecules that defend against oxidative stress. This approach includes compounds like MitoQ,[50] a mitochondrially targeted antioxidant. However, MitoQ

proved to be ineffective in protecting against photoreceptor cell death in the rd1 mouse retina.[5] In addition, antioxidants, reducing ROS production by mitochondria have been tested. For example, dimethylthiourea and PBN (α-phenyl-tert-butylnitrone) are protective in light damage; but no protection was provided to the S334ter rat (summarized in Wenzel et al.[18]). The second approach includes mimicking preconditioning, since mitochondrial ROS production, mitochondrial ATP-sensitive potassium channels, MPTP, and mitochondrial biogenesis all appear to be targets of preconditioning (see review Perez-Pinzon et al.[51]). While preconditioning has been found to be protective against retinal degeneration induced by light,[52,53] it was found to be ineffective in a genetic model.[54] The third approach is neuroprotection. Handa and colleagues have reported that nuclear factor erythroid 2-related factor 2 (Nrf2) signaling is impaired in the aged RPE,[55] and various compounds have been tested for their ability to act as neuroprotectants by upregulating Nrf2.[56,57] However, none of these approaches has been tested rigorously to confirm that the compounds improve mitochondrial function.

Recent work has demonstrated that stabilizing or improving energy metabolism might be of benefit. Rods are known to make rod-derived cone viability factor (RdCVF) and treatment with RdCVF provides ~40% rescue effect for cones, and promotes cone survival by stimulating aerobic glycolysis in these cells.[58] Likewise, Hurley and colleagues have documented the importance of mitochondrial activity and substrates for anabolic activity in photoreceptor survival.[59] Resveratrol, which modulates mitochondrial function and redox biology, has been shown to reduce light-induced retinal degeneration,[60] and MTP-131, a peptide that selectively targets mitochondrial cardiolipin promotes efficient electron transfer, reversed the visual decline in a rodent model of diabetes.[61]

The pharmacological target of CB11 is not clear. Based on our previous data presented at the RD2014 meeting,[46] CB11 was found to both protect against mitochondrial fission by decreasing Drp1, a GTPase that is a member of the dynamin superfamily of proteins and involved in mitochondrial fission, and increasing Mfn2, a GTPase embedded in the mitochondrial outer membrane and involved in mitochondrial fusion. Work is being conducted to identify the target of CB11 in mitochondrial dynamics.

In addition to the relevance to RP, our findings have important implications for ageing and AMD. Alterations in mitochondrial structure and function have been studied in ageing and in AMD. RPE cells isolated from old donor eyes appear to exhibit mitochondrial decay (mitochondrial fission),[10] bioenergetic deficiencies, and weakened antioxidant defenses.[6] Based on the observation that retinal degeneration with very different underlying risk factors (eg, genetics, light damage, smoking, etc.) share this alteration in energy metabolism, we proposed that reduction in energy metabolism is a common feature of photoreceptor dystrophies and that compounds, such as CB11 prevent this decline and serve as a treatment of retinal degeneration.

In summary, as mitochondrial dysfunction is a common feature in most neurodegenerative diseases, identifying compounds that improve mitochondrial structure and function, is paramount for the extension of lifespan of the affected cells and tissues.

Author Contributions

Participated in research design: C.B., Y.K.P., C.C.L., and B.R.

Conducted experiments: Y.K.P., N.P., M.B., C.N., G.B., R.F.C., and C.C.L.

Contributed new reagents or analytic tools: n/a.

Performed data analysis: C.B., Y.K.P., N.P., M.B., C.N., G.B., R.F.C., C.C.L., and B.R.

Wrote or contributed to the writing of the article: C.B., Y.P., R.G.S., and B.R.

Acknowledgments

The authors wish to thank Alison C. Smith, DVM and Roxanna Vaughn from the Department of Comparative Medicine for the access to teaching laboratory swine. The authors thank Charles Smith and Christian Knaak from MUSC for support and assistance with the ChemBridge ionophore screen.

Author Disclosure Statement

No competing financial interests exist.

Funding Information

This study was supported in part by the National Institutes of Health (NIH) (R01EY019320), Department of Veterans Affairs (I01 RX000444, IK6BX004858), Foundation Fighting Blindness (Wynn-Gund Translational Research Acceleration Grant), and the SmartState Foundation of the State of South Carolina. Animal studies were conducted in a facility constructed with support from the NIH (C06 RR015455).

References

1. Daiger, S.P., Sullivan, L.S., and Bowne, S.J. Genes and mutations causing retinitis pigmentosa. *Clin. Genet*. 84: 132–141, 2013.
2. Farber, D.B. From mice to men: the cyclic GMP phosphodiesterase gene in vision and disease. The Proctor Lecture. *Invest. Ophthalmol. Vis. Sci.* 36:263–275, 1995.
3. Travis, G.H., Sutcliffe, J.G., and Bok, D. The retinal degeneration slow (rds) gene product is a photoreceptor disc membrane-associated glycoprotein. *Neuron*. 6:61–70, 1991.
4. Lohr, H.R., Kuntchithapautham, K., Sharma, A.K., and Rohrer, B. Multiple, parallel cellular suicide mechanisms participate in photoreceptor cell death. *Exp. Eye Res*. 83: 380–389, 2006.
5. Vlachantoni, D., Bramall, A.N., Murphy, M.P., Taylor, R.W., Shu, X., Tulloch, B., Van Veen, T., Turnbull, D.M., McInnes, R.R., and Wright, A.F. Evidence of severe mitochondrial oxidative stress and a protective effect of low oxygen in mouse models of inherited photoreceptor degeneration. *Hum. Mol. Genet*. 20:322–335, 2011.
6. He, Y., and Tombran-Tink, J. Mitochondrial decay and impairment of antioxidant defenses in aging RPE cells. *Adv. Exp. Med. Biol*. 664:165–183, 2011.
7. Campello, L., Esteve-Rudd, J., Bru-Martinez, R., Herrero, M.T., Fernandez-Villalba, E., Cuenca, N., and Martin-Nieto, J. Alterations in energy metabolism, neuroprotection and visual signal transduction in the retina of Parkinsonian, MPTP-treated monkeys. *PLoS One*. 8:e74439, 2013.

8. Barot, M., Gokulgandhi, M.R., and Mitra, A.K. Mitochondrial dysfunction in retinal diseases. *Curr. Eye Res*. 36:1069–1077, 2011.
9. Wang, A.L., Lukas, T.J., Yuan, M., Du, N., Handa, J.T., and Neufeld, A.H. Changes in retinal pigment epithelium related to cigarette smoke: possible relevance to smoking as a risk factor for age-related macular degeneration. *PLoS One*. 4:e5304, 2009.
10. Feher, J., Kovacs, I., Artico, M., Cavallotti, C., Papale, A., and Balacco Gabrieli, C. Mitochondrial alterations of retinal pigment epithelium in age-related macular degeneration. *Neurobiol. Aging*. 27:983–993, 2006.
11. Fisher, C.R., and Ferrington, D.A. Perspective on AMD pathobiology: a bioenergetic crisis in the RPE. *Invest. Ophthalmol. Vis. Sci*. 59:AMD41–AMD47, 2018.
12. Ferrington, D.A., Fisher, C.R., and Kowluru, R.A. Mitochondrial defects drive degenerative retinal diseases. *Trends Mol. Med*. 26:105–118, 2020.
13. Tan, E., Ding, X.Q., Saadi, A., Agarwal, N., Naash, M.I., and Al-Ubaidi, M.R. Expression of cone-photoreceptor-specific antigens in a cell line derived from retinal tumors in transgenic mice. *Invest. Ophthalmol. Vis. Sci*. 45:764–768, 2004.
14. Sharma, A.K., and Rohrer, B. Sustained elevation of intracellular cGMP causes oxidative stress triggering calpain-mediated apoptosis in photoreceptor degeneration. *Curr. Eye Res*. 32:259–269, 2007.
15. Farber, D.B., and Lolley, R.N. Cyclic guanosine monophosphate: elevation in degenerating photoreceptor cells of the C3H mouse retina. *Science*. 186:449–451, 1974.
16. Fox, D.A., Poblenz, A.T., and He, L. Calcium overload triggers rod photoreceptor apoptotic cell death in chemical-induced and inherited retinal degenerations. *Ann. N.Y. Acad. Sci.* 893:282–285, 1999.
17. Kunchithapautham, K., and Rohrer, B. Apoptosis and autophagy in photoreceptors exposed to oxidative stress. *Autophagy*. 3:433–441, 2007.
18. Wenzel, A., Grimm, C., Samardzija, M., and Reme, C.E. Molecular mechanisms of light-induced photoreceptor apoptosis and neuroprotection for retinal degeneration. *Prog. Retin. Eye Res*. 24:275–306, 2005.
19. Medrano, C.J., and Fox, D.A. Oxygen consumption in the rat outer and inner retina: light- and pharmacologically-induced inhibition. *Exp. Eye Res*. 61:273–284, 1995.
20. Kooragayala, K., Gotoh, N., Cogliati, T., Nellissery, J., Kaden, T.R., French, S., Balaban, R., Li, W., Covian, R., and Swaroop, A. Quantification of oxygen consumption in retina ex vivo demonstrates limited reserve capacity of photoreceptor mitochondria. *Invest. Ophthalmol. Vis. Sci*. 56:8428–8436, 2015.
21. Ferrick, D.A., Neilson, A., and Beeson, C. Advances in measuring cellular bioenergetics using extracellular flux. *Drug Discov. Today*. 13:268–274, 2008.
22. Griciuc, A., Roux, M.J., Merl, J., Giangrande, A., Hauck, S.M., Aron, L., and Ueffing, M. Proteomic survey reveals altered energetic patterns and metabolic failure prior to retinal degeneration. *J. Neurosci*. 34:2797–2812, 2014.
23. Perron, N.R., Beeson, C., and Rohrer, B. Early alterations in mitochondrial reserve capacity; a means to predict subsequent photoreceptor cell death. *J. Bioenerg. Biomembr*. 45:101–109, 2013.
24. Sharma, A.K., and Rohrer, B. Calcium-induced calpain mediates apoptosis via caspase-3 in a mouse photoreceptor cell line. *J. Biol. Chem*. 279:35564–35572, 2004.
25. Farber, D.B., Park, S., and Yamashita, C. Cyclic GMP-phosphodiesterase of rd retina: biosynthesis and content. *Exp. Eye Res.* 46:363–374, 1988.
26. Anderson, R.E., Maude, M.B., McClellan, M., Matthes, M.T., Yasumura, D., and LaVail, M.M. Low docosahexaenoic acid levels in rod outer segments of rats with P23H and S334ter rhodopsin mutations. *Mol. Vis*. 8:351–358, 2002.
27. Rohrer, B., and Ogilvie, J.M. Retarded outer segment development in TrkB knockout mouse retina organ culture. *Mol. Vis*. 9:18–23, 2003.
28. Ogilvie, J.M., Speck, J.D., Lett, J.M., and Fleming, T.T. A reliable method for organ culture of neonatal mouse retina with long-term survival. *J. Neurosci. Methods*. 87: 57–65, 1999.
29. Pinzon-Duarte, G., Kohler, K., Arango-Gonzalez, B., and Guenther, E. Cell differentiation, synaptogenesis, and influence of the retinal pigment epithelium in a rat neonatal organotypic retina culture. *Vision Res*. 40:3455–3465, 2000.
30. Bandyopadhyay, M., and Rohrer, B. Photoreceptor structure and function is maintained in organotypic cultures of mouse retinas. *Mol. Vis*. 16:1178–1185, 2010.
31. Rohrer, B., Matthes, M.T., LaVail, M.M., and Reichardt, L.F. Lack of p75 receptor does not protect photoreceptors from light-induced cell death. *Exp. Eye Res*. 76:125–129, 2003.
32. Backman, T.W., Cao, Y., and Girke, T. ChemMine tools: an online service for analyzing and clustering small molecules. *Nucleic Acids Res*. 39:W486–W491, 2011.
33. Swindle, M.M., and Smith, A.C. Best practices for performing experimental surgery in swine. *J. Invest. Surg*. 26: 63–71, 2013.
34. Kadam, R.S., Jadhav, G., Ogidigben, M., and Kompella, U.B. Ocular pharmacokinetics of dorzolamide and brinzolamide after single and multiple topical dosing: implications for effects on ocular blood flow. *Drug Metab. Dispos*. 39:1529–1537, 2011.
35. Bero, S.A., Muda, A.K., Choo, Y.-H., Muda, N.A., and Pratama, S.F. Weighted Tanimoto Coefficient for 3D Molecule Structure Similarity Measurement. *arXiv preprint arXiv*:1806.05237. 2018.
36. Sumantran, V.N. Cellular chemosensitivity assays: an overview. *Methods Mol. Biol*. 731:219–236, 2011.
37. Rhoades, J.A., Peterson, Y.K., Zhu, H.J., Appel, D.I., Peloquin, C.A., and Markowitz, J.S. Prediction and in vitro evaluation of selected protease inhibitor antiviral drugs as inhibitors of carboxylesterase 1: a potential source of drug-drug interactions. *Pharm Res*. 29:972–982, 2012.
38. Wills, L.P., Trager, R.E., Beeson, G.C., Lindsey, C.C., Peterson, Y.K., Beeson, C.C., and Schnellmann, R.G. The beta2-adrenoceptor agonist formoterol stimulates mitochondrial biogenesis. *J. Pharmacol. Exp. Ther*. 342:106–118, 2012.
39. Hansch, C., Bjorkroth, J.P., and Leo, A. Hydrophobicity and central nervous system agents: on the principle of minimal hydrophobicity in drug design. *J. Pharm. Sci*. 76: 663–687, 1987.
40. Ogilvie, J.M., and Speck, J.D. Dopamine has a critical role in photoreceptor degeneration in the rd mouse. *Neurobiol. Dis.* 10:33–40, 2002.
41. Ray, A., Sun, G.J., Chan, L., Grzywacz, N.M., Weiland, J., and Lee, E.J. Morphological alterations in retinal neurons in the S334ter-line3 transgenic rat. *Cell Tissue Res*. 339: 481–491, 2010.

42. Chen, J., Makino, C.L., Peachey, N.S., Baylor, D.A., and Simon, M.I. Mechanisms of rhodopsin inactivation in vivo as revealed by a COOH-terminal truncation mutant. *Science*. 267:374–377, 1995.
43. Sung, C.H., Makino, C., Baylor, D., and Nathans, J. A rhodopsin gene mutation responsible for autosomal dominant retinitis pigmentosa results in a protein that is defective in localization to the photoreceptor outer segment. *J. Neurosci*. 14:5818–5833, 1994.
44. Richards, A., Emondi, A.A., and Rohrer, B. Long-term ERG analysis in the partially light-damaged mouse retina reveals regressive and compensatory changes. *Vis. Neurosci*. 23:91–97, 2006.
45. LaVail, M.M., Yasumura, D., Matthes, M.T., Lau-Villacorta, C., Unoki, K., Sung, C.H., and Steinberg, R.H. Protection of mouse photoreceptors by survival factors in retinal degenerations. *Invest. Ophthalmol. Vis. Sci.* 39:592–602, 1998.
46. Beeson, C., Lindsey, C., Nasarre, C., Bandyopadhyay, M., Perron, N., and Rohrer, B. Small molecules that protect mitochondrial function from metabolic stress decelerate loss of photoreceptor cells in murine retinal degeneration models. *Adv. Exp. Med. Biol*. 854:449–454, 2016.
47. Middleton, S. Porcine ophthalmology. *Vet. Clin. North Am. Food Anim. Pract*. 26:557–572, 2010.
48. Paquet-Durand, F., Beck, S., Michalakis, S., Goldmann, T., Huber, G., Muhlfriedel, R., Trifunovic, D., Fischer, M.D., Fahl, E., Duetsch, G., Becirovic, E., Wolfrum, U., van Veen, T., Biel, M., Tanimoto, N., and Seeliger, M.W. A key role for cyclic nucleotide gated (CNG) channels in cGMP-related retinitis pigmentosa. *Hum. Mol. Genet.* 20: 941–947, 2011.
49. LaVail, M.M., Unoki, K., Yasumura, D., Matthes, M.T., Yancopoulos, G.D., and Steinberg, R.H. Multiple growth factors, cytokines, and neurotrophins rescue photoreceptors from the damaging effects of constant light. *Proc. Natl. Acad. Sci. U.S.A*. 89:11249–11253, 1992.
50. Tauskela, JS. MitoQ—a mitochondria-targeted antioxidant. *IDrugs*. 10:399–412, 2007.
51. Perez-Pinzon, M.A., Stetler, R.A., and Fiskum, G. Novel mitochondrial targets for neuroprotection. *J. Cereb. Blood Flow Metab*. 32:1362–1376, 2012.
52. Albarracin, R., and Valter, K. 670 nm red light preconditioning supports muller cell function: evidence from the white light-induced damage model in the rat retina(dagger). *Photochem. Photobiol*. 88:1418–1427, 2012.
53. Lange, C., Heynen, S.R., Tanimoto, N., Thiersch, M., Le, Y.Z., Meneau, I., Seeliger, M.W., Samardzija, M., Caprara, C., and Grimm, C. Normoxic activation of hypoxia-inducible factors in photoreceptors provides transient protection against light-induced retinal degeneration. *Invest. Ophthalmol. Vis. Sci*. 52:5872–5880, 2011.
54. Grimm, C., Wenzel, A., Stanescu, D., Samardzija, M., Hotop, S., Groszer, M., Naash, M., Gassmann, M., and Reme, C. Constitutive overexpression of human erythropoietin protects the mouse retina against induced but not inherited retinal degeneration. *J. Neurosci*. 24:5651–5658, 2004.
55. Sachdeva, M.M., Cano, M., and Handa, J.T. Nrf2 signaling is impaired in the aging RPE given an oxidative insult. *Exp. Eye Res*. 119:111–114, 2014.
56. Zhang, X., Jizhang, Y., Xu, X., Kwiecien, T.D., Li, N., Zhang, Y., Ji, X., Ren, C., and Ding, Y. Protective effects of remote ischemic conditioning against ischemia/reperfusion-induced retinal injury in rats. *Vis. Neurosci*. 31: 245–252, 2014.
57. Li, Y., Zou, X., Cao, K., Xu, J., Yue, T., Dai, F., Zhou, B., Lu, W., Feng, Z., and Liu, J. Curcumin analog 1, 5-bis (2-trifluoromethylphenyl)-1, 4-pentadien-3-one exhibits enhanced ability on Nrf2 activation and protection against acrolein-induced ARPE-19 cell toxicity. *Toxicol. Appl. Pharmacol*. 272:726–735, 2013.
58. Ait-Ali, N., Fridlich, R., Millet-Puel, G., Clerin, E., Delalande, F., Jaillard, C., Blond, F., Perrocheau, L., Reichman, S., Byrne, L.C., Olivier-Bandini, A., Bellalou, J., Moyse, E., Bouillaud, F., Nicol, X., Dalkara, D., van Dorsselaer, A., Sahel, J.A., and Leveillard, T. Rod-derived cone viability factor promotes cone survival by stimulating aerobic glycolysis. *Cell*. 161:817–832, 2015.
59. Chertov, A.O., Holzhausen, L., Kuok, I.T., Couron, D., Parker, E., Linton, J.D., Sadilek, M., Sweet, I.R., and Hurley, J.B. Roles of glucose in photoreceptor survival. *J. Biol. Chem*. 286:34700–34711, 2011.
60. Kubota, S., Kurihara, T., Ebinuma, M., Kubota, M., Yuki, K., Sasaki, M., Noda, K., Ozawa, Y., Oike, Y., Ishida, S., and Tsubota, K. Resveratrol prevents light-induced retinal degeneration via suppressing activator protein-1 activation. *Am. J. Pathol*. 177:1725–1731, 2010.
61. Alam, N.M., Mills, W.C., Wong, A.A., Douglas, R.M., Szeto, H.H., and Prusky, G.T. A mitochondrial therapeutic reverses visual decline in mouse models of diabetes. *Dis. Model Mech*. 8:701–710, 2015.

Received: December 10, 2020
Accepted: March 2, 2021

Address correspondence to:
Dr. Bärbel Rohrer
Department of Ophthalmology
Medical University of South Carolina
167 Ashley Avenue, SEI 614
Charleston, SC 29425
USA

E-mail: rohrer@musc.edu